

TWO DISTINCT RED GIANT BRANCHES IN THE GLOBULAR CLUSTER NGC 288

DONG-GOO ROH¹, YOUNG-WOOK LEE¹, SEOK-JOO JOO¹, SANG-IL HAN¹,
YOUNG-JONG SOHN¹, AND JAE-WOO LEE²

¹*Center for Galaxy Evolution Research and Department of Astronomy, Yonsei University,
Seoul 120-749, Korea ; ywlee2@yonsei.ac.kr*

²*Department of Astronomy and Space Science, Sejong University, Seoul 143-747, Korea*

ABSTRACT

We report the presence of two distinct red giant branches (RGBs) in the globular cluster NGC 288 from the narrow-band calcium and Strömgen b & y photometry obtained at the CTIO 4m Blanco telescope. The RGB of NGC 288 is clearly split into two in the hk [$= (Ca - b) - (b - y)$] index, while the split is not shown in the $b - y$ color. Unlike other globular clusters with multiple populations reported thus far, the horizontal branch of NGC 288 is only mildly extended. Our stellar population models show that this and the presence of two distinct RGBs in NGC 288 can be reproduced if slightly metal-rich ($\Delta[m/H] \approx 0.16$) second generation stars are also enhanced in helium by small amount ($\Delta Y \approx 0.03$) and younger by ~ 1.5 Gyrs. The RGB split in hk index is most likely indicating that the second generation stars were affected by supernovae enrichment, together with the pollutions of lighter elements by intermediate-mass asymptotic giant branch stars or fast-rotating massive stars. In order to confirm this, however, spectroscopy of stars in the two distinct RGB groups is urgently required.

Subject headings: globular clusters: individual (NGC 288) — stars: abundances — stars: evolution

1. INTRODUCTION

Unlike the conventional wisdom, observations made during the past decade have revealed that many globular clusters (GCs) are possessing more than one stellar population. Some of these peculiar GCs, such as ω Cen (Lee et al. 1999; Bedin et al. 2004), M54 (Layden & Sarajedini 1997; Siegel et al. 2007), M22 (Da Costa et al. 2009; Lee et al. 2009a; Marino et al. 2009), NGC 1851 (Han et al. 2009; Lee et al. 2009b; Carretta et al. 2010),

Terzan 5 (Ferraro et al. 2009), and NGC 2419 (Cohen et al. 2010; Di Criscienzo et al. 2011) show evidences of supernovae (SNe) enrichment, indicating that they are relics of more massive primeval dwarf galaxies, rather than being normal GCs. For other GCs with multiple populations, such as NGC 2808 (Piotto et al. 2007), NGC 6388 (Moretti et al. 2009), and M4 (Marino et al. 2008), however, the evidence for the discrete distribution of heavy elements as observed in the RGB of ω Cen is lacking, although spreads in some lighter elements (Carretta et al. 2009, and references therein) and helium (D’Antona et al. 2005; Lee et al. 2005; Piotto et al. 2007; Yoon et al. 2008) are reported. Therefore, the presence of chemical inhomogeneity and multiple populations in these GCs is largely considered due to the pollution from the intermediate-mass asymptotic giant branch (AGB) stars and (or) fast-rotating massive stars (Ventura & D’Antona 2008; Decressin et al. 2007), which is expected even in normal GCs.

Because of their important implications on the hierarchical merging paradigm of Galaxy formation, search for more GCs with dwarf galaxy origin (i.e., with evidence of SNe enrichment) would be extremely important. The purpose of this Letter is to report that NGC 288 is also showing a clear split in the RGB from the narrow-band calcium photometry. This observation is compared with our stellar population models to argue that the two populations are different in terms of overall metallicity, helium, and age by small amounts.

2. OBSERVATIONS AND COLOR-MAGNITUDE DIAGRAMS

Our observations in Ca , b , and y passbands were performed using the CTIO 4m Blanco telescope on 2009 July 27. The telescope was equipped with eight 2048×4096 SITe CCDs, providing a plate scale of $0.27 \text{ arcsec pixel}^{-1}$ and a field-of-view of 36×36 arcmin on the sky. However, since the 4×4 inch filters used in our photometry can not cover the entire field, only four CCD chips located in central region (i.e., chip 2, 3, 6, and 7) covering 2048×2500 pixels per chip were used in the final photometry. The total exposure times for Ca , Strömgen b , and y were 1650, 264, and 132 seconds, respectively, split into short and long exposures in each band. NGC 288 was placed on chip 6, approximately 3.0 arcmin South and 3.1 arcmin East from the CCD center. The IRAF¹ MSCRED Package was used for preprocessing including bias correction and flat fielding. The brightnesses of objects in NGC 288 were measured with the point-spread function (PSF) fitting routine DAOPHOT

¹IRAF is distributed by the National Optical Astronomy Observatories, which are operated by the Association of Universities for Research in Astronomy, Inc., under cooperative agreement with the National Science Foundation.

II and ALLFRAME (Stetson 1987, 1994), and aperture corrections were calculated using the DAOGROW (Stetson 1990). Our photometry in Ca , b , and y passbands were then used to calculate the hk [= $(Ca - b) - (b - y)$] index defined by Anthony-Twarog et al. (1991). The Ca filter in the hk index is meant to measure essentially ionized calcium H and K lines, and the hk index is known to be about three times more sensitive to metallicity than m_1 [= $(v - b) - (b - y)$] index is (Twarog & Anthony-Twarog 1995). The same filter set employed in this observation was extensively used by us in our previous investigations of GCs (Rey et al. 2000, 2004; Lee et al. 2009a,b).

Figure 1 shows color-magnitude diagrams (CMDs) of NGC 288 in $(b - y, y)$ and (hk, y) planes. To examine the CMD features more clearly, magnitude error, chi, sharpness and separation index (Stetson et al. 2003) were used to reject stars with large photometric uncertainty and those affected by blending and adjacent starlight contamination. All stars in the Figure 1 lie within the chip 6, and therefore our CMDs are not subject to any uncertainty stemming from the possible chip to chip variations of the mosaic CCDs. The most remarkable feature of Figure 1 is the presence of two distinct RGBs in the hk vs. y CMD. When measured at $y = 16.5$ mag, the mean separation between the two RGBs is about 0.10 mag in hk index. The discrete distribution shown in RGB, however, is not apparent in the subgiant branch (SGB). Note also that the RGB split is not shown in $(b - y, y)$ CMD. This is most likely because the Ca filter in the hk index is much more sensitive to changes in Ca abundance than other color indices like $b - y$.

Given the small foreground reddening value of $E(B - V) = 0.03$ (Harris 1996) toward NGC 288, it is very unlikely that the differential reddening has caused the double RGBs. Furthermore, in contrast to other color indices, the hk index is known to be insensitive to interstellar reddening, $E(hk)/E(B - V) = -0.12$ and $E(hk)/E(b - y) = -0.16$ (Anthony-Twarog et al. 1991). Therefore, if we adopt the reddening of $E(B - V) = 0.03$, $E(hk) = -0.0036$ is obtained for NGC 288, which is negligible compared to the separation in hk index (~ 0.10 mag) between the two RGBs. Star counts of two subpopulations indicate that the bluer RGB population (“Pop-1”) takes about 60% of the whole population, while the redder RGB population (“Pop-2”) comprises about 40% of total population, in the magnitude interval $y = 16.5 \pm 1.5$ mag. This ratio is not sensitive to the adopted separation index in our photometry.

3. COMPARISON WITH STELLAR POPULATION MODELS

In order to better understand the origin of the RGB split in hk index, and to place constraints on the chemical combinations of two subpopulations, we have constructed stellar

population models based on the latest version of the Yonsei-Yale (Y^2) isochrones (Yi et al. 2008) and HB evolutionary tracks (S.-I. Han et al. 2011, in preparation). Readers are referred to Lee et al. (1990, 1994) and Yoon et al. (2008) for the details of our model construction. Figures 2 and 3 present our synthetic CMDs for NGC 288 in (hk, y) and $(b - y, y)$ planes, respectively. Our models were constructed under three different assumptions regarding the chemical enrichment and age spread in NGC 288. First, we assumed that the second generation population (Pop-2; redder RGB) is more enhanced in metallicity and younger ($\Delta[m/H] \approx 0.16$ dex, $\Delta t \approx 1.5$ Gyr), but not enhanced in helium abundance [hereafter $\Delta Z + \Delta \text{Age}$ model; panel (b) in Figures 2 and 3]. These models match well with the observed CMDs from the MS through the RGB in (hk, y) and $(b - y, y)$ planes. Yet, the models fail to reproduce the HB, as the synthetic HBs are too extended in color including significant numbers of RR Lyraes and red HB stars (HB type² = 0.61), while the observed HB is only mildly extended with mostly blue HB stars (HB type = 0.91). This is because both metal enhancement and younger age in second population move the HB to red in CMD (see Lee et al. 1994). Second, we then assumed that both metal and helium abundances are enhanced ($\Delta[m/H] \approx 0.16$ dex, $\Delta Y \approx 0.03$ dex), but age is constant [hereafter $\Delta Z + \Delta Y$ model; panel (c) in Figures 2 and 3]. These models match well with the observed CMDs from the RGB through the HB in (hk, y) and $(b - y, y)$ planes. However, they can not reproduce the narrow SGB in (hk, y) CMD. Therefore, both $\Delta Z + \Delta \text{Age}$ and $\Delta Z + \Delta Y$ models are in conflict with the observed CMDs of NGC 288.

Finally, we assumed that not only metal and helium abundances are enhanced, but also age is younger in Pop-2 [hereafter $\Delta Z + \Delta Y + \Delta \text{Age}$ model; panel (d) in Figures 2 and 3]. These models are in good agreements with the observations from the MS to the HB. The enhanced metal abundance in Pop-2 makes the RGB split in hk index as observed, while the younger age can explain the narrow and apparently single SGB in (hk, y) CMD. The increase in helium abundance in Pop-2 moves HB bluer (see Lee et al. 2005), almost cancelling out the effects by enhanced metallicity and younger age, making the blue HB only mildly extended with the HB type similar to the observed value (HB type = 0.90). Note that, in our HB simulations, we employ the standard Reimers (1977) mass-loss law and the same mass-loss parameter η for the two subpopulations. Input parameters adopted in our best models (i.e., $\Delta Z + \Delta Y + \Delta \text{Age}$ model) are listed in Table 1. Our models are computed with the same abundance of [CNO/Na/Fe] for both Pop-1 and Pop-2. More detailed models including the possible difference in [CNO/Na/Fe] between the two subpopulations would change the age estimates (see, e.g., Cassisi et al. 2008).

²The HB type is the quantity, $(B-R)/(B+V+R)$, where B, V, and R are the numbers of blue HB, RR Lyrae variable, and red HB stars, respectively (Lee et al. 1994).

4. DISCUSSION

We have shown that the RGB of NGC 288 is split into two distinct sequences. While this is most likely the effect of Ca II H & K lines, it is important to check whether the CN band at $\lambda \approx 3870 \text{ \AA}$ could affect the hk index due to the proximity of the CN band to the blue tail of Ca filter transmission curve. In particular, according to Kayser et al. (2008), lower RGB stars in NGC 288 exhibit CN bimodality that spans about 0.6 dex. In Figure 4a, we have matched their spectroscopic data with our photometry, where we can see that “CN-strong” stars lie well on the redder RGB sequence, whereas “CN-weak” stars are on the bluer RGB. This further suggests that possible contamination of CN band to hk index should be investigated in more detail. It is known that the passband of the narrow band interference filter, such as the Ca filter employed in our photometry, depends on the angle of incidence beam (see Clarke et al. 1975; Lee et al. 2009a). This issue is therefore more relevant when the Ca filter is used with a relatively fast telescope like the prime focus of the CTIO 4m telescope, where the central wavelength drift of the Ca filter is estimated to be about 15 \AA to the shorter wavelength³ (see Figure 4b).

In order to see the influence of CN band on the hk index in our photometry, we have calculated synthetic spectra using the ATLAS 9 model atmosphere (Castelli & Kurucz 2003) for the RGB star at the magnitude level of HB with $T_{\text{eff}} = 4750 \text{ K}$, $\log g = 2.0$ (in cgs unit), $v_{\text{turb}} = 2.0 \text{ km/s}$, and $[\text{Fe}/\text{H}] = -1.6$ (see Lee et al. 2009a Supplementary Information for detail). The typical RGB stars in GCs show an anticorrelation between CN band and CH band strengths and a correlation between CN band and NH band strengths, indicating that the nitrogen controls the CN band strength (Briley & Smith 1993). Therefore, we have compared the synthetic spectra between the stars with normal and enhanced nitrogen abundances (see Figure 4c). We obtain $\Delta hk \approx +0.006$ for $\Delta [\text{N}/\text{Fe}] = +1.0$ dex, which suggests that the influence of CN band on the hk index would be negligible in our photometry⁴. Recently, Sbordone et al. (2011) also reached at a similar conclusion, finding that CNONa anticorrelations have an effect of at most ~ 0.04 mag in the hk color at fixed M_v . Their calculations include not only the direct effects of CN and other absorption bands (NH & CH), but also the effects on the continuum levels in the Ca , b , and y filters.

If the CNONa abundances have only little effects on the hk index as discussed above, which should be confirmed in the forthcoming works, the RGB split discovered in our hk vs. y CMD would indicate a small difference in Ca abundance between the two subpopulations.

³http://www.ctio.noao.edu/instruments/filters/filters_66.html

⁴If we have assumed the wavelength drift of 20 \AA , a similarly small value of Δhk ($\sim +0.009$) is obtained, confirming that this result is not very sensitive to the uncertainty in the value of the wavelength drift.

Since calcium and other heavy elements can only be supplied through SNe explosions, this in turn would suggest that the second generation stars were affected by SNe enrichment, together with the pollutions of lighter elements (such as the enhancement of N and the depletion of O) by intermediate-mass asymptotic giant branch stars or fast-rotating massive stars. Spectroscopy of stars in the two distinct RGB sequences is crucial to confirm the small difference in the abundance of heavier elements suggested in our photometry.

We thank the referee for a number of helpful suggestions. Support for this work was provided by the National Research Foundation of Korea to the Center for Galaxy Evolution Research. This material is based upon work supported by AURA through the NSF under AURA Cooperative Agreement AST 0132798, as amended.

REFERENCES

- Anthony-Twarog, B. J., Twarog, B. A., Heim, E. A., & Caldwell, N. 1991, *AJ*, 101, 1902
- Bedin, L. R., Piotto, G., Anderson, J., Cassisi, S., King, I. R., Momany, Y., & Carraro, G. 2004, *ApJ*, 605, L125
- Briley, M. M., & Smith, G. H. 1993, *PASP*, 105, 1260
- Carretta, E., Bragaglia, A., Gratton, R. G., D’Orazi, V., & Lucatello, S. 2009, *A&A*, 508, 695
- Carretta, E., et al. 2010, *ApJ*, 722, L1
- Cassisi, S., Salaris, M., Pietrinferni, A., Piotto, G., Milone, A. P., Bedin, L. R., & Anderson, J. 2008, *ApJ*, 672, L115
- Castelli, F., & Kurucz, R. L. 2003, in *IAU Symp. 210, Modelling of Stellar Atmospheres*, ed. N. Piskunov, W. W. Weiss, & D. F. Gray (San Francisco: ASP), 20
- Clake, D., McLean, I. S., & Wyllie, T. H. A. 1975, *ApJ*, 43, 215
- Cohen, J. G., Kirby, E. N., Simon, J. D., & Geha, M. 2010, *ApJ*, 725, 288
- Da Costa, G. S., Held, E. V., Saviane, I., & Gullieuszik, M. 2009, *ApJ*, 705, 1481
- D’Antona, F., Bellazzini, M., Caloi, V., Pecci, F. F., Galletti, S., & Rood, R. T. 2005, *ApJ*, 631, 868

- Decressin, T., Meynet, G., Charbonnel, C., Prantzos, N., & Ekström, S. 2007, *A&A*, 464,1029
- Di Criscienzo, M., D’Antona, F., Milone, A. P., Ventura, P., Caloi, V., Carini, R., D’Ercole, A., Vesperini, E., & Piotto, G. 2011, arXiv:astro-ph/1103.0867
- Ferraro, F. R., et al. 2009, *Nature*, 462,483
- Han, S.-I., Lee, Y.-W., Joo, S.-J., Sohn, S. T., Yoon, S.-J., Kim, H.-S., & Lee, J.-W. 2009, *ApJ*, 707, L190
- Harris, W. E. 1996, *AJ*, 112, 1487 (updated in 2010 available on <http://physwww.physics.mcmaster.ca/~harris/mwgc.dat>)
- Kayser, A., Hilker, M., Grebel, E. K., & Willemsen, P. G. 2008, *A&A*, 486, 437
- Layden, A. C., & Sarajedini, A. 1997, *AJ*, 486, L107
- Lee, J.-W., Kang, Y.-W., Lee, J., & Lee, Y.-W. 2009a, *Nature*, 462, 48
- Lee, J.-W., Lee, J., Kang, Y.-W., Lee, Y.-W., Han, S. -I., Joo, S.-J., Rey, S.-C., & Yong, D. 2009b, *ApJ*, 695, 78
- Lee, Y.-W., Demarque, P., & Zinn, R. 1990, *ApJ*, 350, 155
- Lee, Y.-W., Demarque, P., & Zinn, R. 1994, *ApJ*, 423, 248
- Lee, Y.-W., Joo, J.-M., Sohn, Y.-J., Rey, S.-C., Lee, H. -C., & Walker, A. R. 1999, *Nature*, 402, 55L
- Lee, Y.-W., et al. 2005, *ApJ*, 621, L57
- Marino, A. F., Vilanova, S., Piotto, G., Milone, A. P., Momany, Y., Bedin, L. R., & Medling, A. M. 2008, *A&A*, 490, 625
- Marino, A. F., Milone, A. P., Piotto, G., Vilanova, S., Bedin, L. R., Bellini, A., & Renzini, A. 2009, *A&A*, 505, 1099
- Moretti, A., et al. 2009, *A&A*, 493, 539
- Piotto, G., Bedin, L. R., Anderson, J., King, I. R., Cassisi, S., Milone, A. P., Vilanova, S., Pietrinferni, A., & Renzini, A. 2007, *ApJ*, 661, L53
- Reimers, D. 1977, *A&A*, 57, 395
- Rey, S.-C., Lee, Y.-W., Joo, J.-M., Walker, A., & Baird, S. 2000, *AJ*, 119, 1824

- Rey, S.-C., Lee, Y.-W., Ree, C. H., Joo, J.-M., Sohn, Y.-J., & Walker, A. 2004, *AJ*, 127, 958
- Sbordone, L., Salaris, M., Weiss, A., & Cassisi, S. 2011, arXiv:astro-ph/1103.5863
- Siegel, M. H., et al. 2007, *ApJ*, 667, L57
- Stetson, P. B. 1987, *PASP*, 99, 191
- Stetson, P. B. 1990, *PASP*, 102, 932
- Stetson, P. B. 1994, *PASP*, 106, 250
- Stetson, P. B., Bruntt, H., & Grundahl, F. 2003, *PASP*, 115, 413
- Twarog, B. A., & Anthony-Twarog, B. J. 1995, *AJ*, 109, 2828
- Ventura, P., & D’Antona, F. 2008, *MNRAS*, 385, 2034
- Yi, S. K., Kim, Y.-C., Demarque, P., Lee, Y. -W., Han, S. -I., & Kim, D. -G. 2008, *IAU Symposium*, 252, 413
- Yoon, S. -J., Joo, S. -J., Ree, C. H., Han, S. -I., Kim, D. -G., & Lee, Y. -W. 2008, *ApJ*, 677, 1080

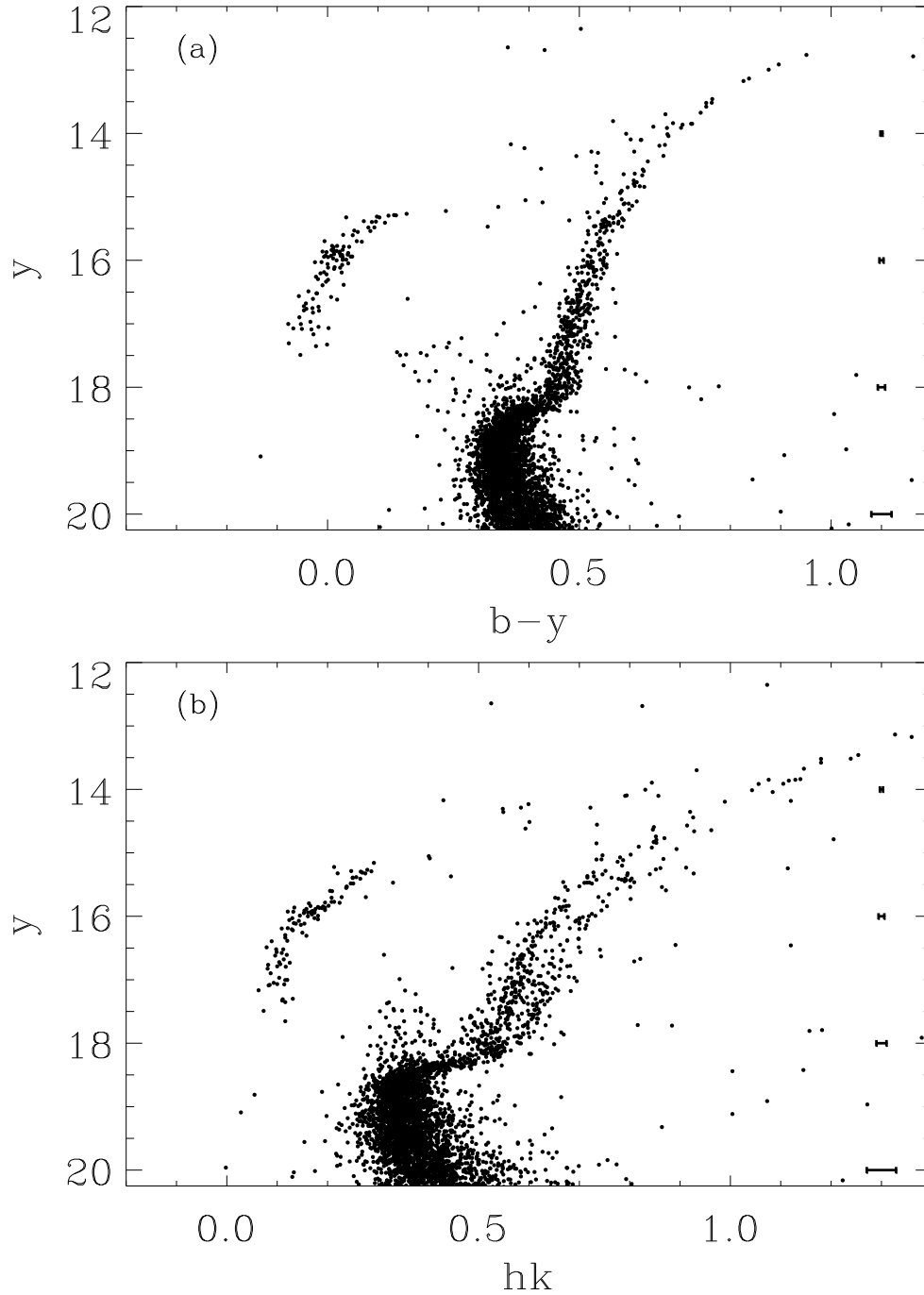


Fig. 1.— Color-magnitude diagrams for NGC 288 from CTIO 4m Blanco Telescope. Note the discrete double RGBs in the hk vs. y CMD. Two RGBs are separated by ~ 0.10 mag in hk index. The reddening vector values are too small [$E(hk) = -0.0036$, $E(b-y) = 0.0225$, and $A_y = 0.093$] to present in this figure.

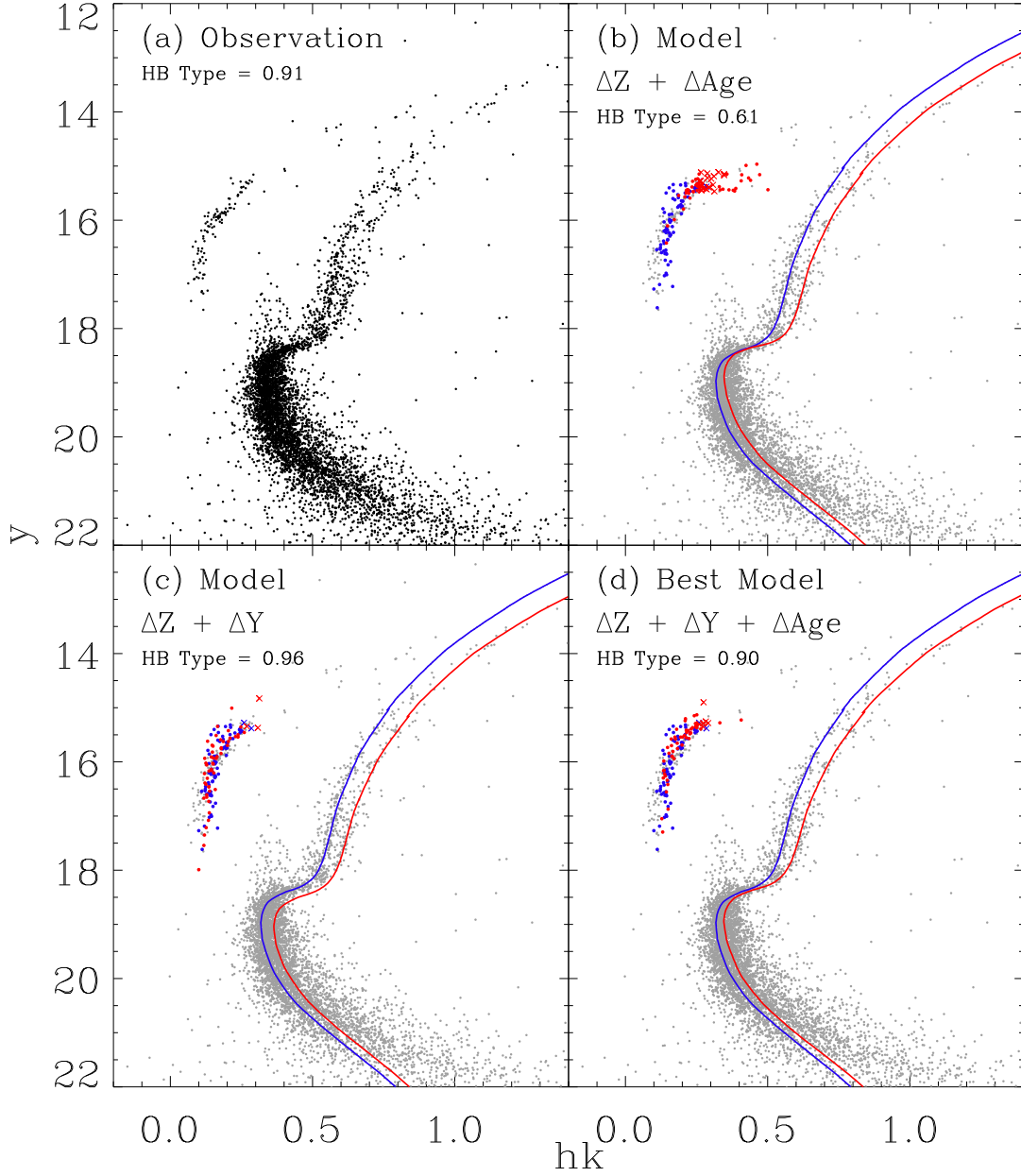


Fig. 2.— Our population models for NGC 288 compared with the observed CMD in hk vs. y plane. In the models, the red lines and symbols are for the metal-rich second generation population, while the blue lines and symbols are for the metal-poor population. The crosses in the models denote RR Lyrae variables. The best match is obtained when metal-rich ($\Delta[m/H] \approx 0.16$) second generation stars are also enhanced in helium by small amount ($\Delta Y \approx 0.03$) and younger by ~ 1.5 Gyrs (see text).

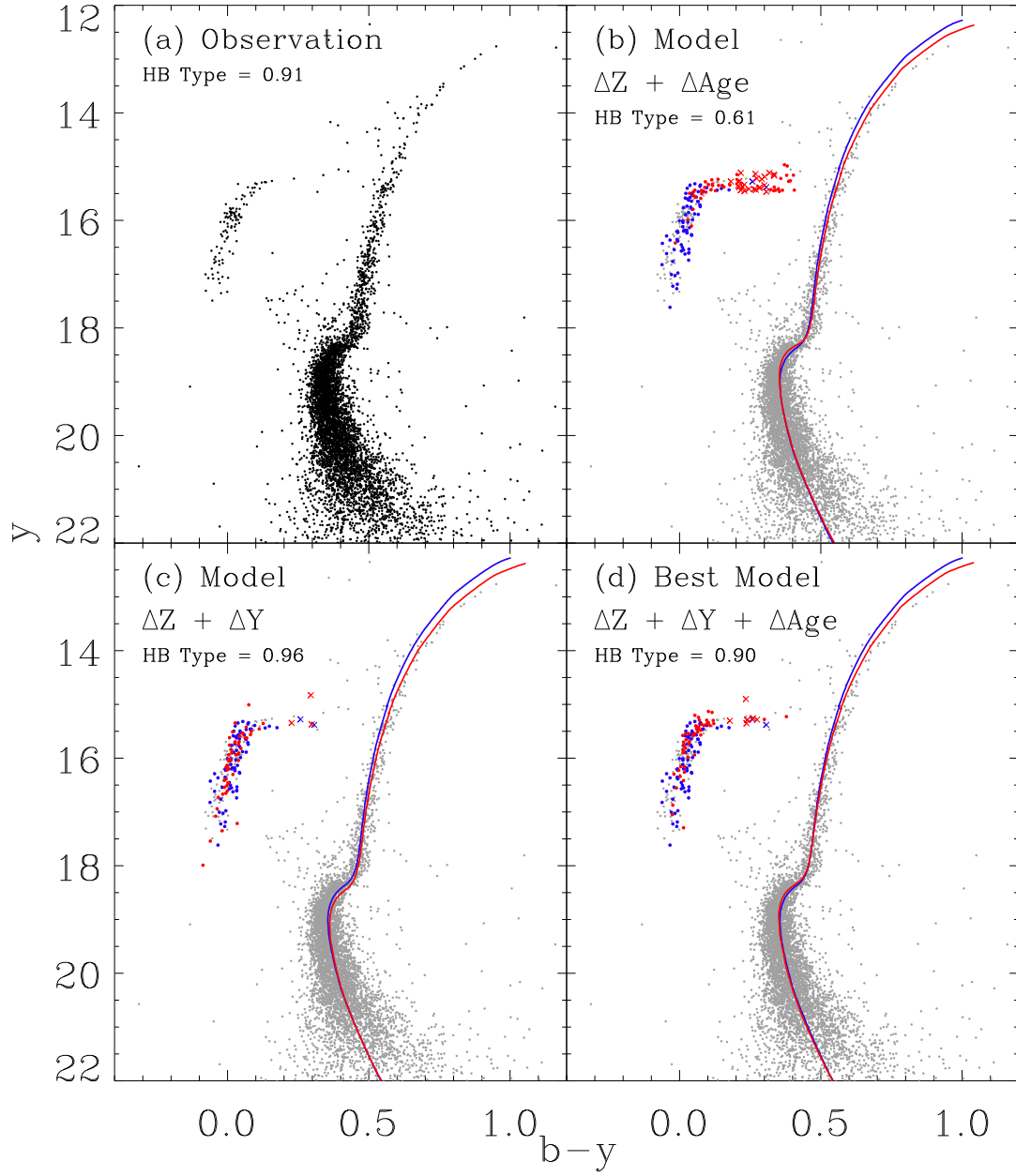


Fig. 3.— Same as Fig. 2, but in $b-y$ vs. y plane.

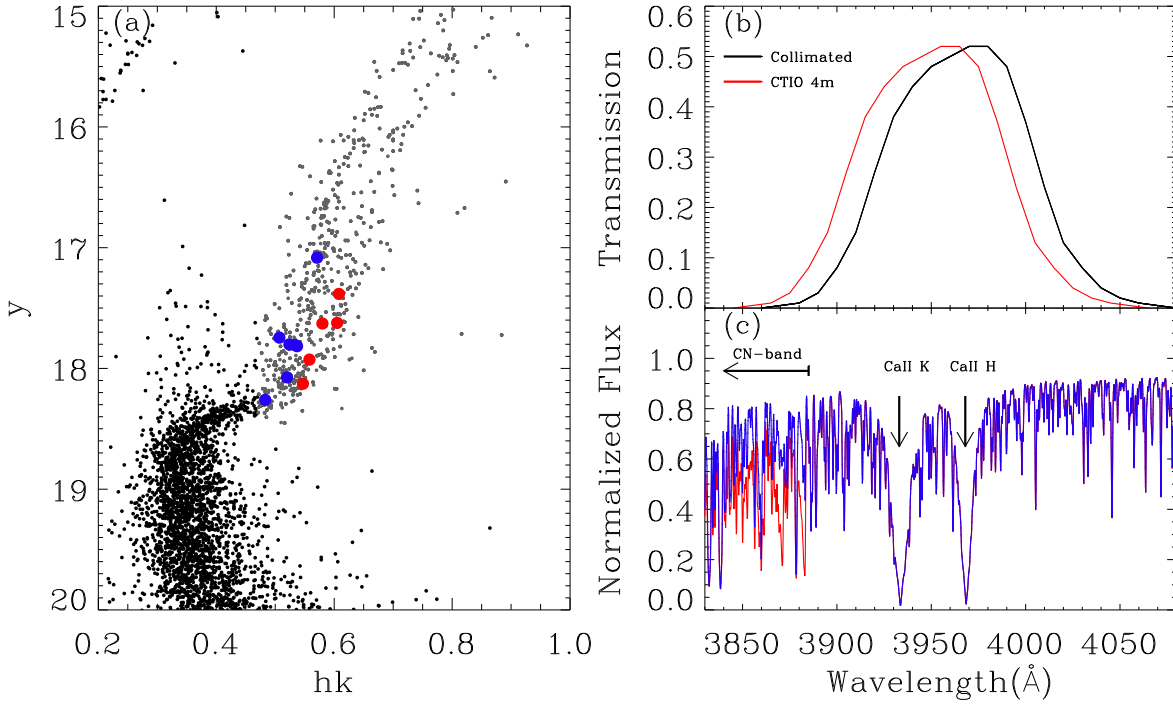


Fig. 4.— (a) Same as Fig. 1b, but zoomed around the SGB and RGB regions in hk vs. y CMD. Denoted by blue and red dots are respectively “CN normal” and “CN strong” stars from Kayser et al. (2008). The CN strength seems to trace the calcium abundance. (b) A comparison of Ca filter transmission functions. The Ca filter at the prime focus of the CTIO 4m telescope is shifted approximately 15 \AA to the shorter wavelength compared to the case of perfectly collimated beam. (c) Synthetic spectra for the CN normal (the blue line) and the CN strong (the red line) RGB stars (see also Supplementary Fig. 1b of Lee et al. 2009a). Although the CN band starting at $\lambda \approx 3885 \text{ \AA}$ lies on the blue tail of Ca filter transmission function, contamination from the CN band appears to be negligible (see text).

Table 1. Input Parameters Adopted in Our Best Simulation of NGC 288

Parameter	Population 1	Population 2
Z	0.00083	0.00121
Y	0.231	0.258
$[\alpha/\text{Fe}]$	0.3	0.3
Age	13.7 ± 0.3 Gyr	12.2 ± 0.3 Gyr
η^{a}	0.53	0.53
ΔM^{b}	0.2179	0.2094
σ_M^{c}	0.020	0.020
Population Ratio	0.6	0.4

^aReimers (1977) mass-loss parameter.

^bMean mass-loss on the RGB (M_{\odot}).

^cMass dispersion on the HB (M_{\odot}).